

## **3D INVERSION OF MT DATA IN GEOTHERMAL EXPLORATION: A WORKFLOW AND APPLICATION TO HENGILL, ICELAND**

Gudni K. Rosenkjaer<sup>1,2)\*</sup> and Douglas W. Oldenburg<sup>1)</sup>

- 1) University of British Columbia, 6339 Stores Road, Vancouver, BC, V6T 1Z4, Canada
- 2) Iceland Geosurvey, Grensasvegur 9, 108 Reykjavik, Iceland

\*Corresponding author: grosenkj@eos.ubc.ca

### **ABSTRACT**

Three-dimensional (3D) inversions of magnetotelluric (MT) data to obtain a resistivity structure of geothermal systems are becoming more accessible with improvements of computer software and hardware. A 3D inversion has clear advantages over lower dimensional inversions, but has high demands of computer power. The motivation for the work discussed in this paper is to develop a workflow for the inversion of magnetotelluric data that facilitates the recovery of high resolution models. By incorporating resistivity structures from inversions with low resolution as starting and background models into a high resolution inversion, the CPU time can be greatly reduced.

The workflow is applied to a 3D inversion of MT data from the Hengill geothermal area in SW Iceland to recover a detailed model with higher resolution of the subsurface resistivity structure. The inverted area is within the South Icelandic Seismic Zone, where fractures and faults provide pathways for geothermal fluids. The recovered resistivity model unveils a similar structure seen in other geothermal systems. A conductive cap is observed close to the surface around the Hengill and Hrómundartindar volcanoes that aligns with the mapped geothermal surface manifestations. Below the cap a resistive core is dominant, particularly beneath the Hrómundartindar volcano. The location corresponds to estimated location of intrusions in the area. A deep conductive layer is seen at a depth of 5 km NW of the Hengill volcano, the nature of which is not fully understood.

### **INTRODUCTION**

Geothermal systems have complex structures that control flow of the fluids within the system. In order to increase our understanding of the properties of the system, it is important to obtain information about their subsurface structure. Geophysical surface methods are commonly used in geothermal exploration and techniques that measure electrical

resistivity have proven to be effective. This is because hydrothermal processes in geothermal systems affect the electrical resistivity of rock units, so models of the subsurface resistivity can be used to identify zones of increased alterations, permeability and porosity. Due to this, the MT method is widely used in geothermal exploration. The method has the potential to reveal the resistivity structure from the near surface down to great depth. In addition to this, field acquisition is logistically simple, and interpretation tools are widely available.

The use of 3D inversion modeling of MT data for geothermal system is a promising technique to obtain reliable high resolution image of the structures in the system. However, obtaining a resistivity model from a 3D inversion is a complex and computationally demanding task. In order to make the inversion of MT data more efficient, a workflow has been developed to speed up the process. The workflow will be discussed and demonstrated on MT data acquired in the Hengill geothermal field in Iceland.

### **THE MT METHOD**

The MT method is a passive electromagnetic (EM) method where orthogonal components of electric and magnetic fields are measured at the surface of the Earth. The source fields are a wide spectrum of EM waves that naturally occur due to lightning discharges and interactions of solar winds and the Earth's magnetosphere. Information about the subsurface resistivity structure, from a few meters to hundreds of kilometers depth, can be interpreted from the collected data. The source wave fields are considered to be plane waves, propagating vertically into the Earth. This assumption holds since refraction of EM waves at the interface between the air and Earth is very high.

### **MT data**

MT data is used in tensor form, as interrelation of the horizontal EM fields at each sound location, such that

$$\begin{bmatrix} Ex \\ Ey \end{bmatrix} = \begin{bmatrix} Z_{xx} & Z_{xy} \\ Z_{yx} & Z_{yy} \end{bmatrix} \begin{bmatrix} Hx \\ Hy \end{bmatrix} \quad (1)$$

The 4 elements in the impedance tensor ( $Z_{xx}$ ,  $Z_{xy}$ ,  $Z_{yx}$ ,  $Z_{yy}$ ) are complex values. The data is collected at discrete locations as a function of time, then processed by Fourier transforms to get frequency dependent data for each location. It is common to present MT data as an apparent resistivity and a phase for the off-diagonal elements of the tensor ( $Z_{xy}$  and  $Z_{yx}$  in Equation (1)) since intuitive understanding of these comes more natural.

When considering a 1D or 2D structure, the on diagonal elements of the impedance tensor ( $Z_{xx}$  and  $Z_{yy}$  in Equation (1)) are generally close to zero, containing little information. In the general 3D case, the on diagonal elements increase in amplitude but are commonly orders of magnitude smaller than the off-diagonal elements.

### **Inversion of MT data**

The goal of an inversion is to recover a resistivity model which produces an MT response that fits the observed data within a given tolerance. This is accomplished using a 3D inversion algorithm. Siripunvaraporn (2011) gives an overview over different algorithms most commonly used in 3D MT inversion. The paper also discusses valuable rules of thumb when performing 3D inversion.

The MT3Dinv inversion code, developed at the University of British Columbia Geophysical Inversion Facility, is used in this paper (Haber, 2000). The inversion problem is solved with an iterative Gauss-Newton procedure, searching for a minimum of the a user defined objective function. The objective function is a weighted sum of the data misfit, and a regularization term added to produce desirable models (smooth and close to a reference model). The inversion process for each frequency is independent and may be solved in parallel on multiple processors for better time efficiency.

The MT3Dinv code requires the user to select an initial model and a reference model that is used in the regularization term. Relevant information about the expected structure can be incorporated into the reference model. The code uses separation of the total electric and magnetic fields to two parts: the primary part is due to a user defined background resistivity model and the secondary part is due to the difference of the actual and background resistivity model.

### **Workflow for 3D inversion of MT data**

Obtaining a high resolution resistivity model with 3D inversion of MT data has high computational cost, both in internal memory required and CPU time. The total number of cells in the model, the number of discrete frequencies selected, and the setup of the inversion have great importance in terms of memory and CPU requirements.

The idea behind the workflow is to conduct the inversion in steps, where results from previous inversion are integrated into subsequent inversions. A subset of the MT data is used at each step, starting with a set of lower frequencies and using a coarse model (low number of cells). The resulting low resolution resistivity model is used as the starting and background models in the subsequent inversion. The model resolution improves by reducing the cell size and a set of frequencies in the medium range of the MT frequency spectrum are used for the subsequent inversion.

The workflow will be discussed in more detail below, where a high resolution model from MT data collected in the Hengill geothermal area in Iceland is inverted. An inversion using a halfspace initial model and using only the off-diagonal element of the data is done for reference. Workflow inversions of off-diagonal and full impedance tensor are discussed and compared to the reference inversion.

### **HENGILL GEOTHERMAL AREA**

The Hengill central volcano is located in SW Iceland, about 30 km from Reykjavik. The Hengill geothermal area is believed to be one of the largest high-temperature geothermal systems in Iceland: 110 km<sup>2</sup> in size with estimated capacity of 690 MWe over 50 years (Franzon et al., 2010)

### **Geological background**

The Hengill geothermal area is commonly considered to consist of 4 sub-fields: Hellisheiði, Nesjavellir, Bitra and Hverahlíð. The Hengill area is located at a triple junction point on the American-Eurasian plate boundary between Western Volcanic Zone (WVZ, an axial rift zone); Reykjanes Peninsula (RP, an oblique spreading ridge); and South Iceland Seismic Zone (SISZ, seismically active transform zone). The main geological structure in the area is a 3-5 km wide and 40 km long fissure/fault swarm with a SSW-NNE strike (blue lines in Figure 1). The greatest volcanic activity is found at the Hengill volcano, leading to a build-up of a tuya mountain from hyaloclastite formations during the glacial period. Supraerial lavas

from interglacial periods are spread over the lowlands surrounding the Hengill volcano.

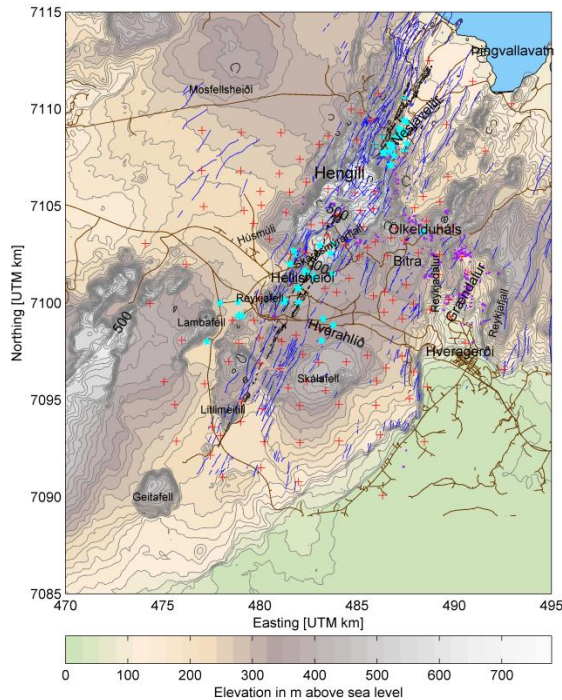


Figure 1: Topographic map of the Hengill geothermal area. Main roads are shown as brown lines, production boreholes are shown as light blue stars, location of MT soundings as red plus sign, surface geothermal manifestations as purple dots, surface fault as blue lines and volcanic fissure as black lines.

The permeability in the Hengill geothermal system is understood to be controlled by boundaries of intrusions and major faults. Basaltic dykes (black lines in Figure 1) from eruptions 5000 and 2000 years ago are found to be major flow channels of geothermal fluids. The upflow zone is considered to be in the Hengill volcano with run-off towards the SW and NE, along the dykes, feeding Helliðshéiði and Nesjavellir geothermal systems (Franson et al., 2005). Surface hydrothermal alteration is found in the Hengill area, mainly in proximity to the volcanic fissure and on an axis from Hengill volcano towards Hvergerði (purple dots in Figure 1).

### **Previous inversions of the MT data**

The MT data in the Hengill geothermal area was collected by various research groups from 2000 to 2006. About 150 MT soundings have been collected, recorded in the frequency range from 300 to 0.001 Hz. For this paper a subset of 131 soundings are used (locations of the MT stations seen as red plus signs in Figure 1). Roughly 280 central loop TEM soundings were collected in the area since 1987 when the method was tested for the first time in Iceland.

The MT data from the Hengill area has been previously inverted. As part of the I-GET project a joint 1D inversion of 146 MT and TEM soundings were done using TEMTD. As well, a 3D inversion of the full impedance tensor of 60 MT soundings was performed using WSINV3DMT inversion code (Arnason et al., 2010). Prior to the 3D inversion, the MT data was corrected for static shift where the static shift multiplier is obtained from a joint 1D inversion of the  $xy$  and  $yx$  MT tensor elements and the TEM data. In Rosenkjaer, (2011) a 3D inversion of the off diagonal elements was done, for MT data that was corrected for static shift and not.

The large scale structures in the resistivity models presented by Arnason et al., (2010) and Rosenkjaer, (2011) largely agree. Both the models are coarse, with horizontal cell dimensions of 1 km by 1 km. The resolution of the models is poor and refinement of the cell sizes is desired.

### **INVERSION OF HENGILL MT DATA**

The MT data from the Hengill geothermal area used for the inversions covers an area of 20 km by 24 km East and North, respectively. The core volume, that we want recover resistivity structure for, extends the area covered with data and down to depth of 10 km.

The goal is to recover a resistivity model where the core volume is discretized with smallest cell sizes of 250x250x50 m in the near surface. All sides of the core volume are padded with cells increasing in size. The topography of the Hengill area is included in the model. The total number of cells in the model is 967,680.

### **3D inversion**

A reference inversion was done, using a best fitting halfspace as a starting model, as is common practice. The off diagonal elements from the 131 MT stations at 11 frequencies spanning 100 to 0.01 Hz were inverted. The level of data misfit was set as of 10% of the data values. The inversion ran for close to 300 hours on 22 Intel Xeon RX5660 CPU's with 2.80 GHz. An internal memory on the order of 64 Gigabytes was required for the inversion.

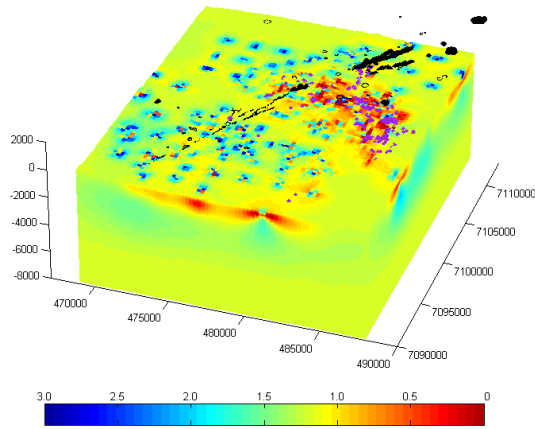


Figure 2. Inversion results using the off-diagonal element and a homogeneous starting model. The volcanic fissures of the Hengill system are shown as black lines and surface geothermal manifestations as purple dots. The coordinates are shown in UTM in zone 27.

The recovered model from the inversion is shown in Figure 2, with the resistivity plotted on a log scale. The main volcanic fissures and the geothermal manifestations mapped on the surface are shown as black lines and purple dots, respectively. A conductive zone can be seen corresponding with the geothermal manifestations, in the area from the Hengill volcano, towards the Hveragerði to the SE. High resistivity is seen surrounding the Hengill volcano, but it is noisy near the data locations. The sensitivity of the high frequency data is highest close to the data locations, so the inversion concentrates structure in these regions and cells with low data sensitivity are left of mostly unchanged. Since the starting model is fairly conductive, the contrast in the surface is locks noise.

### **3D inversion using the workflow**

The goal of the workflow is to facilitate a higher resolution inversion. A reliable starting model speeds up the inversion, using fewer iteration steps to complete the task.

A starting model is built by refining resistivity models from an inversion with lower resolution and models interpolated from 1D inversion of MT and TEM data. In the first step, the core volume is discretized with the smallest cells being  $1000 \times 1000 \times 100 \text{ m}^3$  (horizontal width x height x vertical thickness) in the near surface. In this step, data from 8 frequencies in the range of 1 to 0.01 Hz were used. In the second step, the previous recovered model was used as the starting and background models for an inversion with the smallest cells being  $500 \times 500 \times 75 \text{ m}^3$ . The data was refined as well, using 8 frequencies in the range from 10 to 0.1 Hz. The

final step was to invert 8 frequencies from 100 to 1 Hz for the model with  $250 \times 250 \times 50 \text{ m}^3$  as the smallest cell size. During this step, a 3D model interpolated from 1D of MT and TEM soundings was used to increase the spatial sampling of the resistivity in the near surface. The total CPU time required to build the starting model was on the order of 100 hours, using 16 Intel Xeon RX5660 CPU's with 2.80 GHz for each of the step.

### ***Inversion of off diagonal elements***

Figure 3 presents the recovered model from inversion with a starting model built with the workflow. The data inverted are the same as for the reference inversion. It took less than 7 hours to complete the inversion with the same computer setup as for the previous inversion. The combined time CPU time of about 110 hours is an improvement compared to the 300 hours it took to complete the reference inversion.

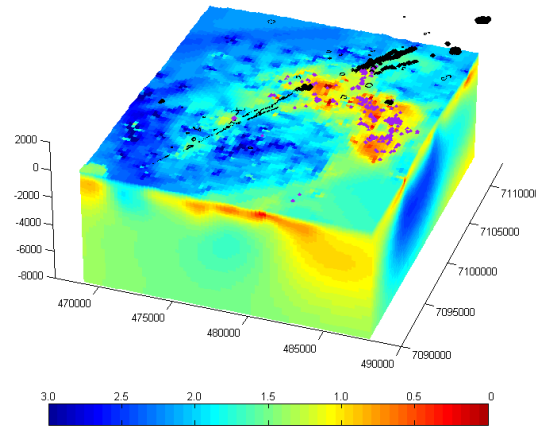


Figure 3. Inversion results using the off-diagonal element and starting model built with the workflow. The volcanic fissures of the Hengill system are shown as black lines and surface geothermal manifestations as purple dots. The coordinates are shown in UTM in zone 27.

There are similarities between the models in Figure 2 and Figure 3. The conductive zone can be seen on the surface of both the models, but the area around the Hengill volcano is better resolved in the workflow inversion. The surrounding area is continuously resistive and the contact between the conductive and resistive zones is better resolved. In the model in Figure 3, a conductive zone can be seen along the volcanic fissures in the SSW-NNE direction.

### ***Inversion of the full impedance tensor***

The resulting model from an inversion of the full impedance tensor is shown in Figure 4. The same frequencies are used as for the previous inversions. The level of data misfit was set as 10% and 20% of the data values for the off-diagonal and the on-

diagonal elements, respectively. It took approximately 80 hours to complete the inversion.

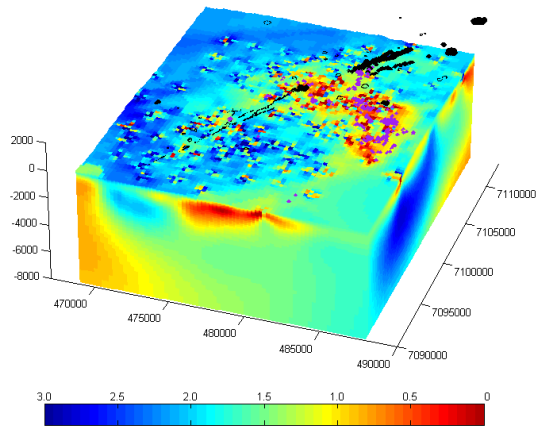


Figure 4. Inversion results of the all the impedance tensor elements and starting model built with the workflow. The volcanic fissures of the Hengill system are shown as black lines and surface geothermal manifestations as purple dots. The coordinates are shown in UTM in zone 27.

The models in Figure 3 and Figure 4 are based on the same starting model and the agreement of the major features is expected. The inversion of the full impedance tensor requires additional time, due to extra iterations needed to fit the data. It is also clear that irregular structures in the surface are needed to fit the full impedance tensor, especially around the data locations.

### Comparison of results

As discussed above, the major surface features are recovered in all the inversions. All the inversions fit the data to comparable level of misfit. Figure 5 has an example of the off diagonal apparent resistivity for one of the MT stations used in the inversion.

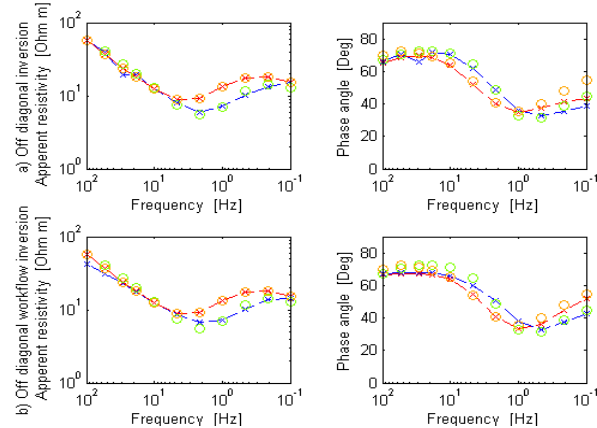


Figure 5. Examples of data fit apparent resistivity and phase for the 3D inversion in a) without the using the workflow and b) with using the workflow. Observed  $xy$  and  $yx$  data are shown as green and orange circles, respectively. The predicted  $xy$  and  $yx$  data are shown as blue and red crosses and lines.

In Figure 5, the observed data is plotted as green and orange circles for  $xy$  and  $yx$ , respectively. The predicted data from the inversion model is plotted with blue and red crosses and lines for  $xy$  and  $yx$ , respectively. In both a) and b) in Figure 5, the curves fit predicted and observed data match well. The data misfit in all the inversion is similar, but features in the models are different. The inversion is an underdetermined problem, and though data sensitivity can cause small scale variations, general appearance should be the same. The surface structure of all the models varies. The noise surface in Figure 2 is an example, where the resistive structure is concentrated close to the data locations, where the sensitivity is highest. However, the general structure of the model is similar, building the confidence in the results.

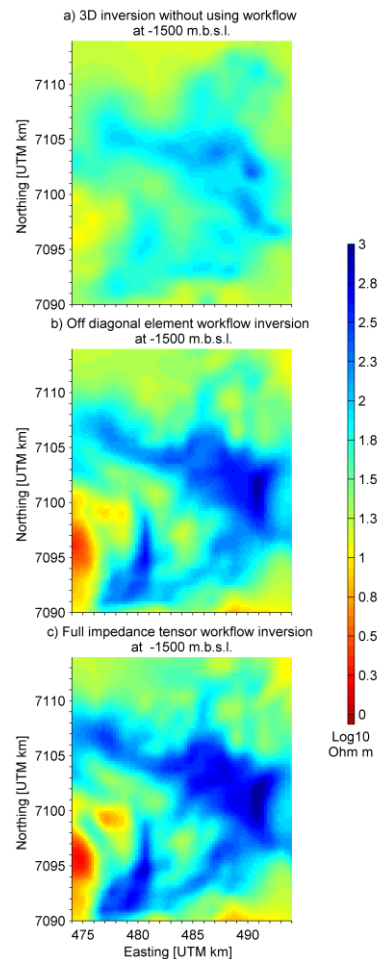


Figure 6. Depth slices at -1500 m.b.s.l. for a) 3D inversion of the off-diagonal elements without using the workflow, b) 3D inversion workflow of the off-diagonal elements only and c) 3D inversion workflow of the full impedance tensor

At increased depth, all the models are smoother and have better refined structures. Figure 6 compares the models at the depth of -1500 m below the sea level. The structure in all the models agrees, but the models

based on the inversion workflow have more refined contacts and better delineation of the structures.

### **DISCUSSION OF RESISTIVITY STRUCTURE**

The main features of the recovered resistivity structure of the Hengill area can be categorized as:

- A conductive cap in the near surface at the Hengill volcano towards the SE. On the outer edges, the surface is resistive.
- Resistive ridges with NW-SE and SW-NE strikes that intersect at the Hengill volcano, coming close to the surface at -500 m.b.s.l. (m below sea-level).
- A deep conductive layer, rising to a depth of -5000m at underneath the Hengill volcano.

The character of the near surface conductive cap and the resistive core are fairly well understood. The conductive cap corresponds to smectite and zeolite hydrothermal alterations, where temperatures are 100-230°C and the geothermal fluid flows in the rock. Resistive rocks at the surface relate to unaltered and cold rocks. At depth within the system where temperatures exceeding 250°C, chlorite and epidote alteration become dominant increasing the resistivity.

The nature of the deep conductive layer, commonly seen underneath geothermal systems, is not fully understood. This conductive layer likely corresponds to the heat source of the the geothermal system.

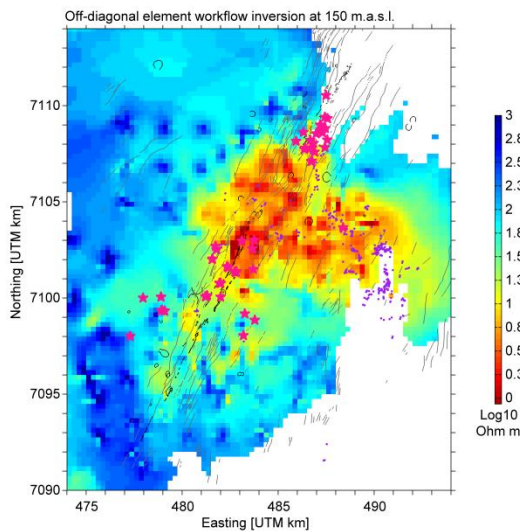


*Figure 7. Depth slice of resulting resistivity model at 150 m.a.s.l. The volcanic fissures are shown as black lines, surface faults are shown as gray lines, surface geothermal manifestations as purple dot and wells are shown as pink stars.*

A depth map at 150 m.a.s.l. is shown in Figure 7. A conductive area is clearly visible around the Hengill which agrees well with the mapped geothermal manifestations at the surface (purple dots). Unaltered and cold rocks are resistive and encircle the conductive zone. The conductive cap primarily extends towards the SE from the Hengill volcano but an axis along the main fissure and fault strike can be seen. The less dominant conductive rim stretches from the Hengill volcano to the SW.

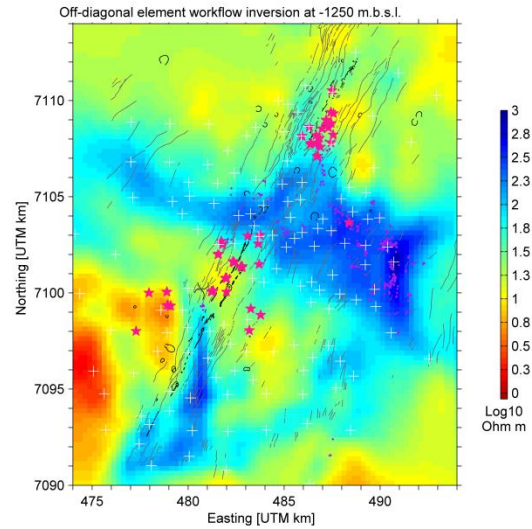


*Figure 8. Depth slice of the resulting resistivity model at -1000 m.b.s.l. The volcanic fissures are shown as black lines, surface faults are shown as gray lines, surface geothermal manifestations as purple dot and wells are shown as pink stars.*

In Figure 8, at -1250 m.b.s.l., a resistive ridge with a NW-SE strike can be seen beneath the conductive cap in the near surface (Figure 7). The resistive ridge mainly seen at the Eastern side of the Hengill volcano but a thin resistive tongue is extends towards the NW. No surface manifestations are mapped nor does the conductive cap reach the surface in this area.

The well locations in the area are shown as pink stars in Figure 7 and Figure 8. Most of the wells are located in the main fissure swarm, at Nesjavellir and the Hellisheiði fields. In relation to the resistive core, most of the wells are drilled on the edge of the structure.

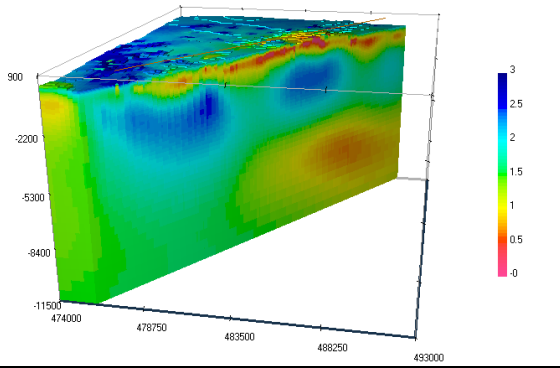


Figure 9. Cross section along the fissure swarm intersecting the Hengill volcano.

South of the Hengill volcano, a second resistive body is seen, near the end of the cross section in Figure 9. The two resistive structures appear to be connected, forming a resistive layer of varying depth and thickness. The zone between the structures has low data coverage, so determination of the structure is low. The resistive layer rises closest to the surface underneath the Hengill volcano and west of Skálafell, where the layer is thicker. Underneath the resistive layer, a conductive layer appears. The conductive layer is especially apparent north of the Hengill volcano.

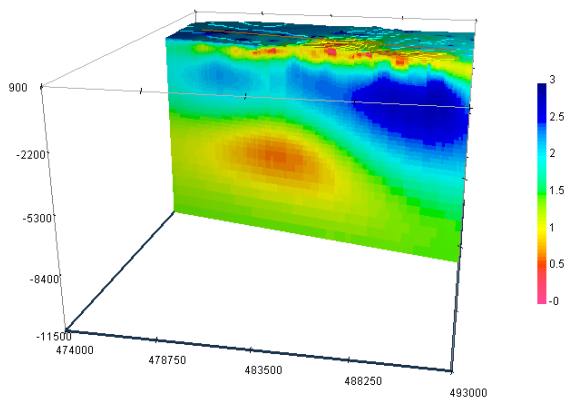


Figure 10. Cross section across the fissure swarm intersecting the Hengill volcano.

A cross section across the main geologic strike direction is shown in Figure 10. The conductive cap reaches the surface at the Hengill volcano. The resistive layer has a greater intensity and thickness on the Eastern side. The depth of the deep conductive layer decreases while the conductivity increases towards the NW.

The recovered resistivity structure agrees with the conceptual model that has been developed for the Hengill geothermal system. The upflow zone of

geothermal fluids is believed to be associated with the Hengill volcano and the volcanic fissures provide flow paths to the SW and NE. The extent of the conductive cap and the underlying resistive core agrees with the surface geothermal manifestations that are mainly SE of the Hengill volcano.

The area SE of the Hengill volcano hosts the older volcanic complexes of Grænidalur and Hrómundartindar. The area is within the stress fields of the SISZ and majority of seismic events originate here. A seismic episode from 1991 to 2001 is related to inflation due to a magmatic intrusion at 6 to 7 km depth below Hrómundartindar (Sigmundsson et al., 1997). The increased thickness and intensity of the resistive body SE of Hengill volcano (Figure 8 and Figure 10) is likely related to the increased temperature and permeability from the intrusive bodies.

## CONCLUSION

3D inversion of MT data proves to be an effective method to gain better understanding of the complex structures of geothermal systems. The resistivity model obtained from the inversion coincides with the geometry of the hydrothermal alteration of the system. The alteration is governed by the temperature and fluid flow in the system - valuable properties when it comes to geothermal power production. Obtaining a detailed resistivity model from the inversion has high computational costs, both in CPU time and memory. By employing a workflow, which obtains the resistivity model in a step wise procedure significantly decreases the computational demands.

When the inversion workflow is applied to MT data from the Hengill geothermal area, it recovers the classic resistivity structure of geothermal systems. A near surface conductive cap extends from the Hengill volcano to the Hrómundartindar volcano. The cap coincides with hydrothermal alterations, where smectite and zeolite clays decrease the resistivity relative to unaltered rocks that surround the volcano. Under the conductive cap a resistive core is the governing structure, particularly underneath the Hrómundartindar volcano. The large resistive structure is located in the same area as known intrusive bodies and zone of increased seismic activity.

High resolution 3D inversion shows its potential for imaging complex structures of geothermal systems. Employing the workflow significantly decreases the CPU memory and time demands, making the process

more practical and recovering a detailed resistivity model.

Siripunvaraporn, W., (2011), "Three-Dimensional Magnetotelluric Inversion: An Introductory Guide for Developers and Users", *Surveys in Geophysics*, **33**, 5-27.

### **ACKNOWLEDGEMENTS**

This work was carried out at the University of British Columbia with funding provided by Geothermal Research Group (GEORG) in Iceland.

### **REFERENCES**

Farquharson, C. G., Oldenburg, D. W., Haber, E., and Shecktmann, R., 2002, "An algorithm for the three-dimensional inversion of magnetotelluric data", *72<sup>nd</sup> Annual International Meeting*.

Franzson, H., Gunnlaugsson, E., Árnason, K., Sæmundsson, K., Steingrímsson, B., and Harðarson, B. S., 2010, "The Hengill Geothermal System, Conceptual model and Thermal Evolution", *Proceedings World Geothermal Congress 2010*, Bali, Indonesia, 25-29 April 2010.

Franzson, H., Kristjánsson, B. R., Gunnarsson, G., Björnsson, G., Hjartarson, A., Steingrímsson, B., Gunnlaugsson, E., and Grímsson, G., 2005, "The Hengill-Hellisheiði Geothermal Field. Development of a Conceptual Geothermal Model", *Proceedings World Geothermal Congress 2005*, Antalya, Turkey, 24-29 April 2005.

Gasperiškova, E., Newman, G., Feucht, D., and Arnason, K. (2011), "3D MT Characterization of Two Geothermal Fields in Iceland", *Geothermal Research Council Transactions*, **35**, 1667-1671.

Haber, E., Ascher, U. M., Oldenburg, D. W., 2000, "On optimization techniques for solving nonlinear inverse problems", *Inverse Problems*, **16**, 1263-1280.

Rosenkjear, G. K., 2011, "Electromagnetic methods in geothermal exploration. 1D and 3D inversion of TEM and MT data from a synthetic geothermal area and the Hengill geothermal area, SW Iceland", *MS thesis*, Faculty of Earth Sciences, University of Iceland.

Sigmundsson, F., Einarsson, P., Rögnvaldsson, S., Foulger, G. R., Hodgkinson, K. M., Thorbergsson, G., 1997, "The 1994-1995 seismicity and deformation at the Hengill triple junction, Iceland: Triggering of earthquakes by minor magma injection in a zone of horizontal shear stress", *J. Geophys. Res.*, 102(B7), 15151-15161.